

Shear Damage Control in Assessing Flat Slab Bridge Decks

Candy CCE, Technical Director Structures - Maunsell WA

Pressley JS, Associate Director – Maunsell WA

Walton BL, Structural Engineer - Maunsell WA

Sanjayan JG, Associate Professor - Monash University and Consultant to Maunsell

SYNOPSIS

Full scale destructive load testing of flat slab Bridge No. 1049, over Baandee Lakes on Great Eastern Highway was commissioned in 2002 by Main Roads Western Australia. Two bending tests and two punching shear tests were carried out. The 5 x 7.5m span reinforced concrete flat slab bridge is typical of many similar structures.

Comparisons are made between the current empirically based treatment of punching shear and general shear in codes, and the observations from the tests.

Rationally based axial/shear stress models of each of the tested spans are proposed, examining the uncracked “slab compression field” in the concrete. Correlation is described between the indicated positions of local breaches of the Mohr/Coulomb stress envelope and the actual positions of diagonal shear cracking observed in the tests, at the failure loads.

For punching shear failure over column supports, predictions from a recently published (Dec 2002) theoretical plasticity model are compared with the ultimate punching shear test results.

Conclusions reached include a rational approach to shear assessment of flat slab bridge decks.

1 GENERAL SHEAR RESPONSE OF BRIDGE NO. 1049

A companion paper titled “Destructive Load Testing of Bridge No. 1049 – Analyses, Predictions and Testing” describes four individual tests and the loading configurations.

The Austroads Bridge Design Code (ABDC, Ref 1), like many other design codes, treats flexural shear in slabs as if they were wide beams. This type of shear is referred to in the text as general shear (as opposed to punching shear over support columns).

1.1 General Shear Observations

Two bending tests were carried out on the 5 span flat slab bridge deck. One test had a single T44 tandem axle configuration near midspan of an end span and offset to one side. The other had dual T44 tandem axles near midspan of the other end span, also offset from centre.

For each of the bending tests, ultimate failure was by sudden general shear cracking in the concrete at load magnitudes on the plateaux of the measured load / deflection curves.

The ultimate failure mode for each bending test (single T44 and dual T44's side-by-side) was a shallow angled shear failure surface, L-shaped in plan, extending around the loaded area, but not near lines of support. The failure surface patterns are shown in Fig 1 below.

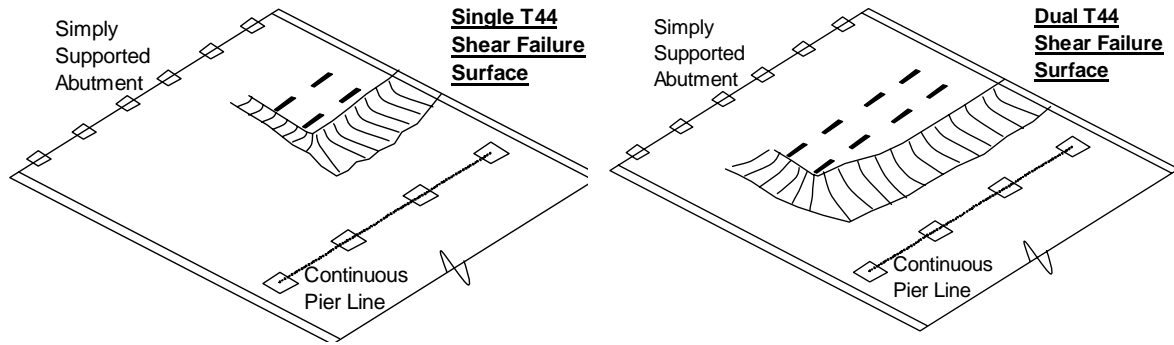


Figure 1: Shear Failure Surfaces for End Span Tests

The applied live load at failure for the single T44 tandem axle test was 2,490 kN. For the dual T44 test it was 3,901 kN.

1.2 ABDC Prediction of General Shear Response

1.2.1 Applied Ultimate Shear Forces and ABDC Capacities

In most codes general shear capacity is considered as the product of a shear stress and the effective vertical area of concrete at a section, to the depth of tensile reinforcement. This approach implies that at the collapse state an ultimate shear stress is smeared to a uniform value across an effective vertical failure surface, by mechanisms of aggregate interlock etc. For slabs $\leq 300\text{mm}$ thick, and where “shear failure could occur across the entire width or over a substantial width” the ABDC allows a minimum shear stress of $0.17 \sqrt{f'_c} b d_0$, which is independent of the quantity of tensile reinforcement. This originates from the longstanding imperial units expression, $2 \sqrt{f'_c} b d_0$, from the 1962 ACI-ASCE Committee 326, and which is based on tests on beams with an average 2.2% tensile reinforcement. The above expression was used to calculate a “minimum” capacity for the constant thickness deck. This applies to any section along the span and is evaluated (without a ϕ factor) in Table 1 below.

A second empirical expression in the ABDC for general “beam” shear capacity, with longitudinal reinforcement considered, no shear reinforcement, and the appropriate β_1 , β_2 and β_3 evaluated for Bridge No. 1049, is shown below and evaluated in Table 1 ($f'_c = 32.5 \text{ MPa}$).

$$V_u = 1.48 \sqrt[3]{(f'_c A_{st} / b d_0)} b d_0, \text{ for sections further than } 2 d_0 \text{ from a support, and double this for sections within } d_0 \text{ from a support}$$

Location	LL + DL Shear Force at Failure (kN)		ABDC Shear Capacity (kN)	
	Single T44 Test	Dual T44 Test	across 0.8 x deck width	across full width
2 d_0 away from abutment	1,151	1,604	1,958	2,447
At zone of minimum tensile reinforcement	1,807	2,745	1,556	1,945
2 d_0 from pier piles	1,953	2,911	2,243	2,804
At all sections, “minimum” capacity			1,929	2,411

Table 1: Applied Shear Forces and Capacities

1.2.2 Discussion on Ultimate Shear Forces and ABDC Minimum Capacity

The predicted minimum capacity using the current ABDC approach and the expression $0.17 \sqrt{f'_c} b d_0$, is quite accurate for the single T44 test and an assumed 0.8 x deck width acting (7% over-prediction). For the dual T44 test there is a conservative under-prediction of 12% with the full deck width acting. It is tempting to conclude that this simplified “minimum” empirical approach is quite acceptable but, as pointed out below, it conceals the true shear behaviour and could lead to unsafe practice.

- Because reinforcement areas are not considered, the requirement is to check shear only near lines of support, where DL + LL shear effects are maximum, or at locations dictated by changes in slab thickness (should this be the case for other bridges). For Bridge No. 1049 the test shear forces were slightly greater adjacent to the piers (due to dead load), so using this approach, shear failure would be expected locally, near these supports. This did not occur. In each test the deck failed in shear between the loaded area and the pier support, with a shallow angled failure surface through the slab thickness, spreading longitudinally over more than 1 metre, and laterally over more than the load width. The shear failure surface displayed a very shallow orientation.
- The transverse width of deck that acts in shear at a particular section, and for a particular load position, should be accurately assessed since it has a significant effect on calculated capacity. The ABDC does not give guidance on this, and it is not rational to simply choose either the full deck width or an estimated 0.8 x deck width (as “substantial”).
- Collins and Kuchma (3), Gasteble and May (5) and Reineck et al (7) have highlighted that the expression $0.17 \sqrt{f'_c} b d_0$, for shear capacity, is unsafe. Reference is made to Bazant and Kazemi (2) who have described relevant fracture mechanics principles and the size effect. The former two papers infer that the coefficient 0.17 could vary between 0.05 and 0.25, depending upon the size of the shear surface. Reineck’s statistical evaluation concludes that the ACI equation is unsafe. There is potentially very wide variability, and further careful assessment is required.

1.2.3 Discussion on Shear Forces and ABDC Capacity with Reinforcement

The predicted capacities using the current ABDC “beam” approach, considering tensile reinforcement, provide quite conservative under-predictions between 14% and 29% of actual tested shear forces, for the zones of minimum reinforcement. The formulae have been empirically derived, and because assumptions are required for the transverse shear width the degree of conservatism is appropriate. The approach is more consistent with contemporary research, but lacks the fracture based size effect component, involving depth and shear span.

There is a further outstanding issue that detracts from the rationality of the approach, this being the correct matching of theoretical shear failure surfaces, and their associated stresses, with the actual failure surfaces observed in tests.

1.3 Current Approaches to General Shear

As discussed in Section 1.2.1 current considerations of general shear assume that vertical surfaces have a smeared average shear stress acting over the effective depth to tensile reinforcement. Gasteble (5) proposes a formula for shear capacity that includes reinforcement area and shear span as well as breadth, effective depth and concrete strength

(approximate cube root). This approximates (within 10%) a recently published CEB-FIP formula for a range of beam depths but departs in the $\leq 300\text{mm}$ slab thickness range. Zararis (12) and Gastebled (5) propose curved or angled shear failure surface models with tensile reinforcement through the surface. The proposals are based on shear tests of simply supported beams where the bottom reinforcement is in tension. Duthinh (4) correlates the modified compression field theory of Vecchio and Collins (11) with other research, as it applies to curved shear surfaces.

The resultant conclusions and proposals contain formulae where the shear area is the product of breadth and effective depth, with an empirically derived smeared ultimate shear stress. The approaches referenced above are derived from and apply mainly to simply supported beams with predominantly plane stress conditions (rather than plane strain), no transverse effects and span to depth ratios somewhat less those for Bridge No. 1049.

A significant difference between the Bridge No. 1049 tests and those of other researchers is span continuity. Unlike in simply supported beam tests, the shear failure surfaces in the two spans tested extended through the plane of contraflexure, between sagging at midspan and hogging over a line of pier supports, as shown in Fig 2. The concrete at both the top and bottom fibres of the wide, shallow-angled shear failure surfaces was in horizontal compression, not tension/compression as in simply supported tests. Therefore the reinforcement was acting in compression near the bottom of the failure surface as well as near the top. The models by other researchers have considered only tensile reinforcement acting.

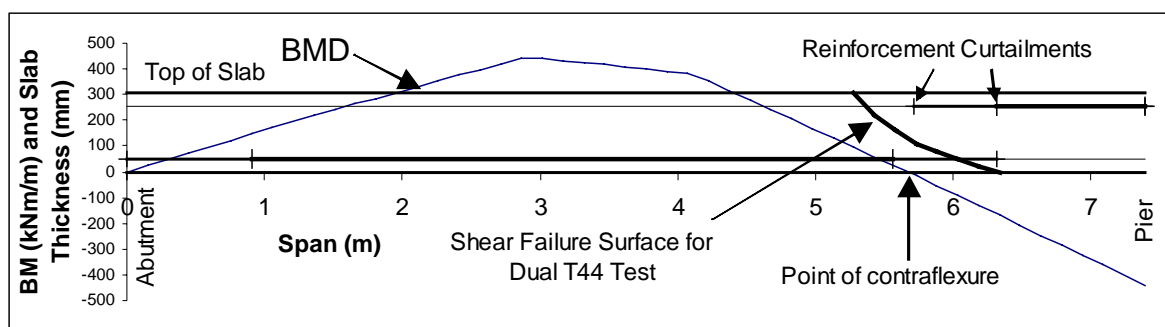


Figure 2: Longitudinal Shear Failure Conditions

A closer examination of the concrete stress fields was therefore required and this shed new light on the shear behaviour. The following Section 1.4 describes the “slab compression field” methodology which was used to understand why the tested concrete failed as it did.

1.4 Rational Approach to Shear, Using Slab Compression Field Methodology

The fundamentals that underpin the slab compression field methodology are described in Sections 1.4.1 to 1.4.3. This methodology is not the same as the modified compression field theory of Vecchio and Collins (11), which is applicable to plane stress, reinforced concrete membranes and not to this essentially plane strain, non-shear-reinforced concrete problem.

1.4.1 Concrete Stress State and Shear Crack Propagation

Flexural cracking in reinforced concrete slabs is a ductile phenomenon with two post-elastic phases in the load / deflection curve. The first is softening due to flexural crack propagation and debonding of reinforcement near cracks, and the second has the addition of tensile reinforcement yielding. By contrast, shear cracking in reinforced concrete slabs without shear

stirrups is a non-ductile phenomenon. It happens very quickly and is dependent on the ambient stress state in the concrete.

Reinforced concrete in bending is usually considered to be in a flexurally cracked state, with zones of cracked and zones of uncracked concrete, these two zones having quite different shear stiffness. It is therefore reasonable to consider that bending moments are sustained by the cracked reinforced section, and that shear forces are sustained by the uncracked portion of the section, which is in compression. This is supported by the principle that load is attracted to the stiffer parts of a structure, and hence shear stress is attracted to the uncracked, stiffer compression field, rather than spreading through the full section depth. Aggregate interlock will attract some shear stress to the cracked portion but this is considered negligible at the ultimate strength limit state, where flexural cracking is extensive and cracks are quite wide.

The shear stress distribution on a vertical plane, in the compression field, is assumed to be parabolic, according to first principles. This is shown in Fig 3 for the slab compression field (left). The current ABDC provisions (right) assume a uniform distribution throughout the effective depth.

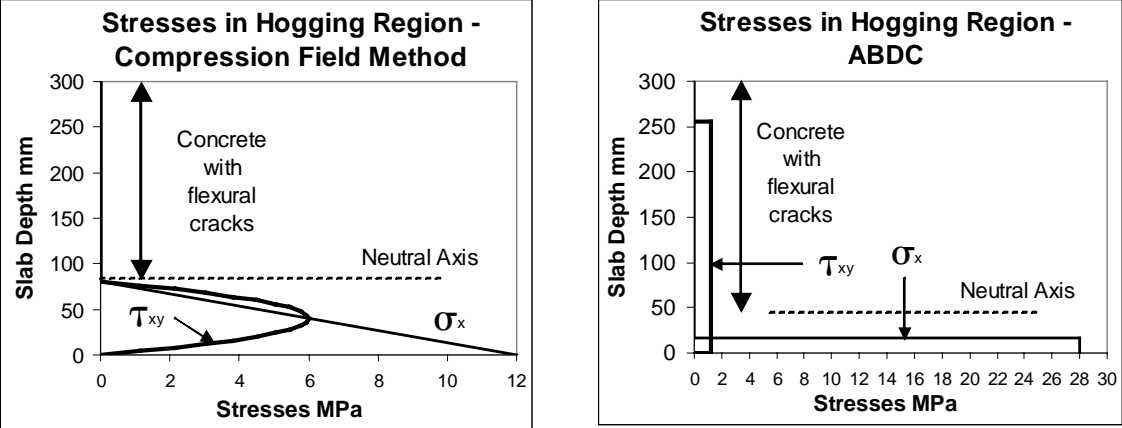


Figure 3: Stress Distributions through Slab Depth

This parabolic shear stress distribution in the compression field is supported by Tureyen and Frosch in their 2003 paper (10) where very good agreement has been established between theory and 370 shear test results.

It is therefore necessary to consider concrete compressive (bending) and shear stresses together throughout the slab compression field.

1.4.2 Mohr Circles and Coulomb Failure Line

Two-dimensional (2D) stress analysis is used for the main span areas. It is much easier to view and understand on paper, and little accuracy is lost in omitting the third (transverse) stress field dimension. It has therefore been preferred for this study ahead of full 3D analysis.

At every point in the 2D longitudinal slab compression field there will be a longitudinal compressive stress from bending. Since for most slabs the concrete compressive strength is not significantly exceeded at the outer fibre, it is reasonable to consider “balanced sections” with triangular compressive stress distributions, rather than rectangular stress blocks. The true distribution may well be parabolic for the short term heavy bridge loading expected, but the

linear variation is considered conservative and reasonably accurate, as discussed below. This is supported by (10).

Concrete strength in two dimensions may be represented by Mohr Circle theory and a limiting Coulomb Failure Line (envelope), which is parabolic about the X-axis. The Coulomb Failure Line is unique for a particular concrete strength, at a particular point, with a particular tensile strain. It is constructed using a mean (best estimate from test cores) uniaxial compressive strength, $f_c = 32.5$ MPa and a uniaxial tensile strength, f_t (discussed below).

Paultre and Mitchell (6), in their analysis of representative national codes and over 200 results from various researchers, conclude that the mean modulus of rupture from a large number of tests, $f_r = 0.94 \sqrt{f'_c}$. Using the commonly used relationship $f'_c = f_c - 8$ MPa, $f_r = 4.65$ MPa. This is equivalent to $f_r = 0.82 \sqrt{f_c}$. After calibrating against the single and dual T44 test results, a value was found for $f_t = 0.8 \sqrt{f_c}$, which approximates the generally accepted upper limit for modulus of rupture and is taken as the starting point for maximum tensile strength.

Fig 4 below shows how f_c and f_t are used to construct the Coulomb Failure Line. Any two-dimensional stress state within the particular concrete that produces a Mohr Circle intersecting the Coulomb Failure Line, at one or two points, will initiate crack growth and damage. This is illustrated in Fig 4, where the increased $\sigma_x = 10$ MPa in the figure on the right “protects” the concrete from shear related damage, for the same shear stress.

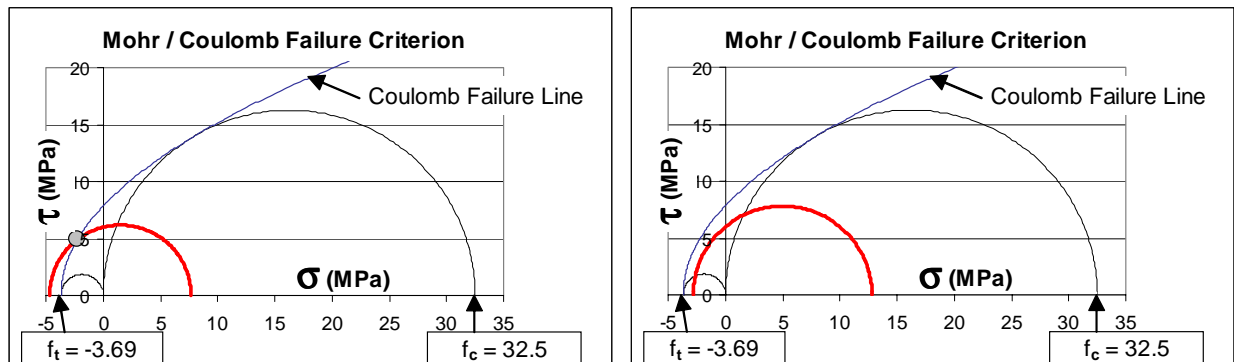


Figure 4: $\sigma_x = 3$ MPa, $\tau = 6$ MPa (damage-left), $\sigma_x = 10$ MPa, $\tau = 6$ MPa (no damage-right)

As shear is spread widthwise across a wider surface, away from the load, the “average” shear capacity for that width decreases due to tensile strain softening. The Coulomb Failure Surface is therefore adjusted accordingly to account for this averaged lower stress capacity.

The tensile strength of the concrete in Bridge No. 1049, in a combined state of compression and shear, was assumed to range from 4.65 MPa down to 3.69 MPa, depending on how much tensile strain had occurred due to shear stress distribution across the width. The stresses are represented by algorithms in the analysis spreadsheet and are in the range of the tension softening models reported in the literature for small tensile strains.

1.4.3 Distribution of Bending Moment and Shear Force

Because the analysis was carried out on a longitudinal 2D stress field, reasonable assumptions were required for transverse distribution of bending and shear, as well as for the longitudinal distribution of moments from span to internal pier line. The tests were intended for ultimate bending response with maximum redistribution. A programmed iterative approach was therefore used in the spreadsheet analysis, as described below.

A constant width of influence was assumed at the T44 load location within which a uniform transverse distribution of longitudinal bending moment and shear force was assumed. This width was considered constant from the location of the T44 tandem axle, back to the simply supported abutment. A linearly varying width of influence was allowed towards the continuous pier line. Because of reinforcement curtailment, allowance was also made for a critical location between the T44 load and the pier, after which the width returned to constant up to the pier (as shown in Fig 5). Between the end of the width of influence and the far (kerb) edge of the deck, the bending moments were considered to vary linearly to zero, whereas the shear forces were considered to reduce more rapidly according to a parabolic law.

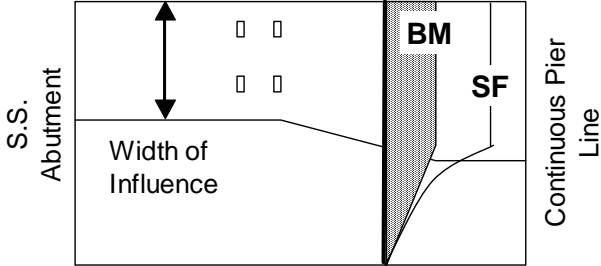


Figure 5: Assumed Widths of Influence and Distributions of Moment and Shear

The spreadsheet algorithm was designed to balance the unit moments in sag and hog at pier and midspan by varying the widths of influence.

1.4.4 Shear Damage Checks

The above methodology produces a rational representation of the longitudinal 2D stress state in the concrete on a typical line through the loaded width. From this it is possible to carry out the Mohr Circle checks described above to identify any local areas of shear damage. The following Section 1.5 describes the outcomes of this approach as applied to Bridge 1049.

1.5 Slab Compression Field Methodology Applied to Test Results

Fig 6 below illustrates the rational approach with a longitudinal section of the end span for the single T44 load test (exaggerated vertical scale). The shaded areas denote the flexurally cracked parts of the sections. The angled solid line is the theoretical cracking plane in the concrete compression field where the Coulomb Failure Line is first breached at 100% failure load. The angle shown (exaggerated vertically) is at 90° to the line of principal tension as derived from the Mohr Circle. The length of the line is scaled to the stress magnitude.

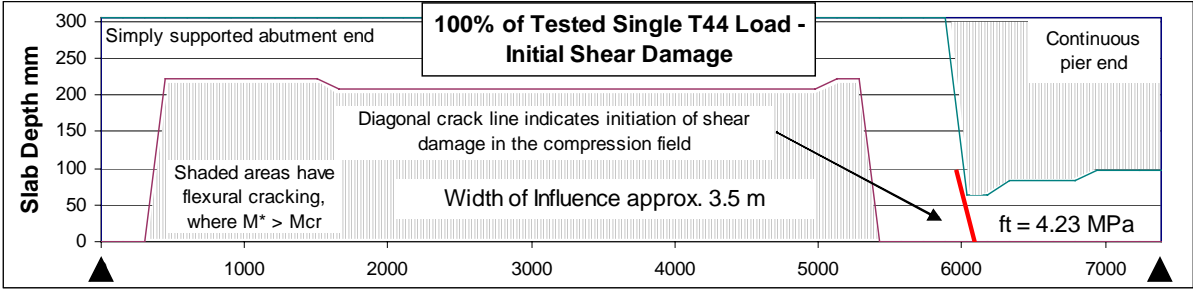


Figure 6: Analysis Model of Initiation of Shear Damage – Single T44 Test

For the dual T44 test Fig 7 below shows three locations of theoretical damage at 118% of the ultimate tested dual T44 load. The significance of this plot is that the predicted theoretical damage only occurs where the actual shear failure surface propagated through the thickness in the test, and nowhere else (see Fig 2).

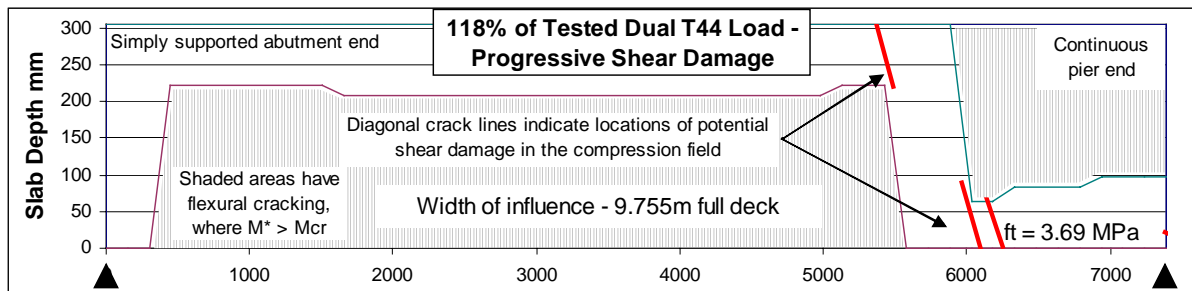


Figure 7: Analysis Model of Progressive Development of Shear Damage – Dual T44 Test

The theoretical width of influence for this test (9.755m) is greater than the loaded width (6.0m) and there is a range of principal tensile strains in the compression field, across the width of influence. This results in a reduction of the average tensile stress capacity from 4.65 MPa to 3.69 MPa, according to a stress/strain algorithm in the spreadsheet. The stress state at the first damage location is shown in Fig 4 (left diagram). The reason that shear damage does not occur nearer the continuous pier is that greater compressive stresses from hogging moments “protect” the concrete (see Section 1.4.2).

There is a zone of minimum bending moment across the point of contraflexure where no flexural cracking is assumed. The shear stresses in this zone are spread throughout the slab thickness and are theoretically much less than in the adjacent compression fields on either side. The question arises as to how the shear failure surface propagates through this zone. In reality there will be a smooth transition of the stress field into the zone and the damaged concrete on either side will drive crack propagation through the zone according to fracture mechanics principles. Investigation of this is to be the subject of a subsequent paper.

1.5.1 Summary of the Approaches to Shear Stress and Areas Acting

At the ultimate strength limit state the current ABDC considers general shear forces to be uniformly distributed over the effective cracked section depth and over an unspecified width of deck. The empirically derived average shear stress capacities (without a ϕ factor) are in the order of 1 MPa for the concrete in Bridge No. 1049.

The slab compression field methodology considers a parabolic distribution of shear stress with the relevant depth being the uncracked part of the balanced concrete section to the neutral axis. Stresses are distributed uniformly over a width of deck consistent with the transverse distribution of ultimate bending moment required for equilibrium. The rationally derived shear stress capacities for Bridge No. 1049 (without a ϕ factor) are governed by concrete tensile strength in the range 4.65 MPa down to 3.69 MPa, depending on how much transverse distribution is required for bending moment equilibrium. This approach pinpoints areas of potential shear related damage which may accumulate with successive vehicle load applications. It has a rational basis, requiring only correlation and verification against a range of test results.

surface has been empirically derived from a body of test results.

In 2002 Salim and Sebastian (8) proposed an alternative rational approach.

2.4 Punching Shear – Alternative Rational Approach

The Salim and Sebastian approach (8) uses a rigid-perfectly plastic concrete model for the calculation of punching shear capacity. Effectiveness factors are applied to reduce the maximum tested uniaxial compressive and tensile strengths of the concrete in order to approximate the overall ductile characteristics of the slab.

The paper presents two different equations for each of the tension and compression effectiveness factors allowing four possible combinations (see Ref 8 for the equations and their derivation). The effectiveness factors need to be “determined by calibration against test data”. Two methods are given in (8) for determining the punching shear capacity, an upper bound formula that assumes a curved failure generatrix, and a simplified approach that adopts a straight line failure generatrix. Fig 8 indicates these.

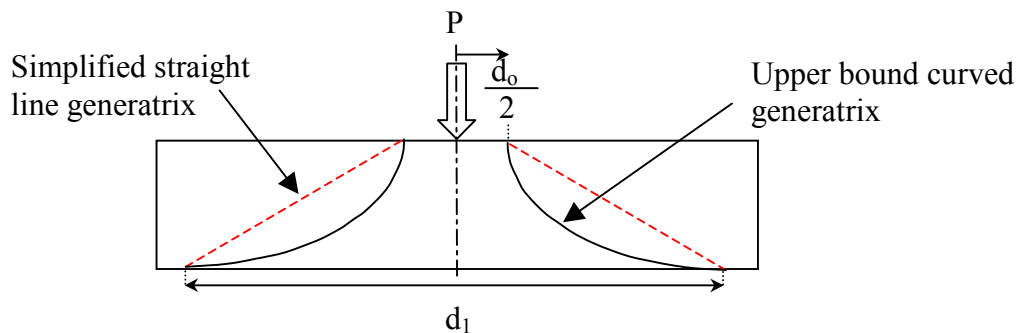


Figure 8: Sketch of Failure Generatrix Proposed by Salim and Sebastian (8)

Unlike in the ABDC approach, the failure surfaces are inclined at shallower angles than 45° .

In order to investigate which combination best fitted the test results, the capacities predicted using the extreme values, in four combinations, were calculated and are shown in Table 2.

Effectiveness factor combinations	Predicted collapse load (kN)	
	Simplified	Upper-bound
Equations 9a, 10a	1,608	1,297
9a, 10b	1,837	1,615
9b, 10a	2,466	1,990
9b, 10b	2,816	2,477
Test Loads	1,570 and 1,690	

Table 2: Comparison of Salim and Sebastian (8) and Test Loads.

In their paper, the authors suggest adopting the simplified approach using the effectiveness factor equations 9a and 10a. This rational approach would under-predict the capacity by 1%.

Discussions with the authors on the wide range of values that were calculated from the method (see Table 2), highlighted membrane effects as an important action that influences punching shear capacity. Membrane action was not investigated in their original approach, and indeed much of the research carried out to date has been on “mushroom head” laboratory

specimens that lack the lateral constraints acting in real slabs. It is understood that these tests have produced somewhat conservative empirical constants.

After investigating this further in 2003, Salim and Sebastian (9) attempted to quantify the effects of lateral restraint by installing hoop reinforcement in flat slab test specimens. From these results and a review of other experimental data they concluded that, “the punching shear load will be significantly increased when the slab edges are restrained against lateral movement”. This does not necessarily mean the physical edges of a slab area, but the edges of a punching shear perimeter that would be laterally constrained by significant widths of slab beyond. Correlating the restraint offered by hoop reinforcement to the actual restraint in a large concrete slab is a complex task and no attempts have been made during this study, since the Salim and Sebastian 2003 paper (9) has only recently been published.

2.5 Symmetry and Load Distribution in Punching Shear – a Caution

Bridge decks are subjected to heavy rolling loads which approach column and pile heads from one side. The practice of assuming the full perimeter surface around the column head, as if the design load were placed in an ideal symmetrical position, may not be sufficiently safe. Further work is required on the average effective tensile stresses that would govern shear in this non-symmetrical case, where a wide range of tensile strains could result in a significant reduction in shear capacity because of strain softening effects.

The statically indeterminate and non-linear nature of the slab-pile system results in a degree of inexactness in determining pile head forces, which will vary from structure to structure, depending upon soil, pile spacings etc. Safety and reliability factors should reflect this.

3 CONCLUSIONS

- The “minimum” shear strength for slabs, given in the ABDC as $V_u = 0.17 \sqrt{f'_c} b d_0$ is considered to be unsafe as it conceals the shear stress behaviour and omits some potentially critical parameters.
- The general “beam” shear and punching shear provisions in the ABDC, whilst conservative for Bridge No. 1049 (capacities 14% to 29% less than tested), are empirically based and assume arbitrary shear lengths (or perimeters). A more accurate rationale is required to match observed ultimate shear behaviour.
- The ABDC shear provisions consider the full effective depth of the cracked section and low levels of uniformly distributed shear stress. These are inconsistent with observed test behaviour, current knowledge of concrete shear/tensile capacity and Mohr/Coulomb failure criteria.

The following approach is proposed for general and asymmetrical punching shear in slabs:

1. For analysis use plate, grillage or simplified transverse distribution models with cracked section properties. Allow an appropriate amount of ultimate moment redistribution to derive accurate shear forces and associated bending moments per unit width, for a number of load positions and potential critical stress locations.

2. Use Mohr/Coulomb criteria in the uncracked compression field, with balanced section axial compressive bending stresses together with parabolically varying shear stresses. Limit local peaks of combined stress to the Coulomb Failure Line with $f_t = K \sqrt{f_c}$, where K depends on distribution and is chosen using reliability theory to be <0.8 .

For symmetrical punching shear use the Salim and Sebastian recommended method after establishing appropriate reliability checked reduction factors for capacity.

ACKNOWLEDGEMENT

The authors wish to acknowledge Main Roads WA for their initiative in proposing and funding the research programme, and their permission to use material in this paper.

REFERENCES

- 1 AUSTROADS 1992, "92 AustRoads Bridge Design Code", AustRoads, , AP-15, 1992.
- 2 BAZANT, ZP, KAZEMI, MT, "Size Effect on Diagonal Shear Failure of Beams without Stirrups", ACI Structural Journal 88-S29, May-June 1991.
- 3 COLLINS, MP, KUCHMA, D; "How Safe Are Our Large, Lightly Reinforced Concrete Beams, Slabs, and Footings?", ACI Structural Journal 96-S54, July-August 1999.
- 4 DUTHINH, D; "Sensitivity of Shear Strength of Reinforced Concrete and Prestressed Concrete Beams to Shear Friction and Concrete Softening According to Modified Compression Field Theory", ACI Structural Journal 96-S56, July-August 1999.
- 5 GASTEBLED, OJ; MAY, IM; "Fracture Mechanics Model Applied to Shear Failure of Reinforced Concrete Beams without Stirrups", ACI Structural Journal 98-S18, March-April 2001.
- 6 PAULTRE, P, MITCHELL, D, "Concrete International", May 2003.
- 7 REINECK, KH; KUCHMA, DA; KIM, SK; MARX, "Shear Database for Reinforced Concrete Members without Sheer Reinforcement", ACI Structural Journal 100-S26, March-April 2003.
- 8 SALIM, W. and SEBASTIAN, W. M.; "Plasticity Model for Predicting Punching Shear Strengths of Reinforced Concrete Slabs," ACI Structural Journal, 99-S84, November-December 2002.
- 9 SALIM, W; and SEBASTIAN, W. M.; "Punching Shear Failure in Reinforced Concrete Slabs with Compressive Membrane Action", ACI Structural Journal 100-S50, July-August 2003.
- 10 TUREYEN, AK, FROSCHE, RJ, "Concrete Shear Strength: Another Perspective", ACI Structural Journal 100-S63, September-October 2003.
- 11 VECCHIO, FJ; COLLINS, MP; "The Modified Compression-Field Theory for Reinforced Concrete Elements Subjected to Shear", ACI Journal 83-22, March-April 1986.
- 12 ZARARIS, PD, "Shear Strength and Minimum Shear Reinforcement of Reinforced Concrete Slender Beams", ACI Structural Journal 100-S22, March-April 2003.